Mathematical Biosciences and Engineering

http://www.aimspress.com/journal/MBE

MBE, 17(4): 3998−4017.
DOI: 10.3934/mbe.2020221
Received: 28 February 2020
Accepted: 26 May 2020
Published: 01 June 2020

Research article

Hybrid support vector machine optimization model for inversion of tunnel transient electromagnetic method

Xiao Liang[1,2], Taiyue Qi[1,2,]*, Zhiyi Jin[1,2] and Wangping Qian[1,2]

[1] Key Laboratory of Transportation Tunnel Engineering, Ministry of Education, Chengdu 610031, China
[2] School of Civil Engineering, Southwest Jiaotong University, Chengdu 610031, China

* **Correspondence:** Email: qitaiyue85@126.com; Tel: +8617345852651.

Abstract: The transient electromagnetic method (TEM) can effectively predict adverse geological conditions, and is widely used in underground engineering fields such as coal mining and tunneling. Accurate evaluation of adverse geological features is a crucial problem that requires urgent solutions. TEM inversion is an essential tool in solving such problems. However, the three-dimensional full-space detection of tunnels and its inversion are not sufficiently developed. Therefore, combining a least-squares support vector machine (LSSVM) with particle swarm optimization (PSO), this paper proposes a tunnel TEM inversion approach. Firstly, the PSO algorithm is adopted to optimize the LSSVM model, thus overcoming the randomness and uncertainty of model parameter selection. An orthogonal test method is adopted to optimize the initial parameter combination of the PSO algorithm, which further improves the accuracy of our PSO-LSSVM model. Numerical simulations are conducted to generate 125 sets of original data. The optimized PSO-LSSVM model is then used to predict certain values of the original data. Finally, the optimization model is compared with conventional machine learning methods, and the results show that the randomness of the initial parameters of the PSO algorithm has been reduced and the optimization effect has been improved. The optimized PSO algorithm further improves the stability and accuracy of the generalization ability of the model. Through a comparison of different machine learning methods and laboratory model tests, it is verified that the optimized PSO-LSSVM model proposed in this paper is an effective technique for tunnel TEM detection inversion.

Keywords: transient electromagnetic method; inversion method; hybrid support vector machine; particle swarm optimization

1. Introduction

The extensive application of underground engineering has placed increased emphasis on geological problems such as water-filled faults, karst caves, fracture zones, and other potential disasters. The transient electromagnetic method (TEM) is an effective means of predicting unfavorable geological conditions. This method has unique advantages in detecting specific geological bodies, effectively reducing and preventing accidents [1]. For example, Kanta et al. [2] studied the geological characteristics of Crete, an island in the Mediterranean Sea, using TEM and obtained the hydrogeological and geometric characteristics of a local aquifer. Further, Kalisperi et al. [3] used a transient electromagnetic sounding network to survey the aquifer, and identified the zones of salination of the groundwater. They confirmed that the aquifer had been degraded by saline intrusion, which likely occurs as the result of fractures in a fault zone in Crete. Vallianatos et al. [4] studied the fracture system of Geropotamos, Crete, using TEM, allowing them to obtain the law of late electromagnetic response and propose a local multi-range empirical index.

TEM inversion can identify the characteristic parameters of adverse geological bodies, such as size, distribution, and conductivity. To date, many scholars have researched transient electromagnetic inversion. For example, Pavlov and Zhdanov [5] derived 3D electromagnetic inversion using a linear approximation, while Cheng et al. [6] performed an inversion analysis based on the finite element method [6] and Zhou et al. [7] proposed an iterative inversion method based on finite-difference time-domain forward analysis. Sun and Li et al. [8] developed a correction method for the resistivity subtraction based on the superposition principle of the transient electromagnetic field. Numerical methods proved that their technique could remove most of the influence of tunnel boring machines and retain a resistivity curve that was consistent with the real trend [8]. Xue et al. [9] proposed the S-inversion method to forecast water-filled faults during tunnel excavation based on the second derivative of the conductivity. Model simulations and experimental results confirmed the accuracy of their approach [9].

The above inversion methods are of considerable significance in the application of TEM, but there are still some limitations. Firstly, one- and two-dimensional inversion techniques are relatively mature, but there has been little research on three-dimensional inversion [10–11]. Secondly, the above methods are mainly used for surface detection, rather than tunnel detection. There are some differences between tunnel detection and surface detection. For instance, surface detection occurs in the half-space range, whereas TEM tunnel detection is in the full space, and so full-space effects must be considered. Moreover, the numerical calculation method is complicated. Finally, the selection of inversion parameters depends on the specific case and involves considerable uncertainties. Therefore, it is necessary to study three-dimensional full-space TEM tunnel detection and inversion.

The maturity of computer algorithms and the extensive application of machine learning provide new ideas for tunnel TEM inversion. Machine learning allows the fundamental laws of problems to be identified through deep learning, offering unique advantages for solving nonlinear and complex problems. The application of machine learning to civil engineering has been widely studied. Cho [12] used artificial neural networks to analyze slope stability problems, while Xue employed a support vector machine (SVM) algorithm for slope stability analysis [13]. Rostami also used SVM to analyze the energy consumption of shield tunnels [14], before Zhang et al. applied LSSVM to the sensitivity analysis of tunnels [15].

TEM inversion is a coupled multi-factor problem that is challenging to solve analytically. Therefore, this study tackled the inversion problem through machine learning. First, the basic TEM theory and characteristics of tunnel detection were studied to determine the characteristic parameters that affect inversion. On this basis, the basic theory of LSSVM models and PSO algorithms were studied, and an optimized PSO-LSSVM model was developed. Inversion predictions were carried out based on laboratory test data. Finally, the inversion effect of the PSO-LSSVM model was verified through comparisons with conventional machine learning methods.

2. Theory of full-space TEM

2.1. Fundamental theory

TEM transmits a pulsed magnetic field to the formation of interest using a transmitter such as a loop power supply. During the interval of the pulsed magnetic field, the secondary eddy current field is observed by a coil and other receiving devices.

When TEM is applied to ground surveys, the transmitter excites an induced eddy current in the underground medium, and the receiver obtains the response signal of the secondary eddy current field in the underground half-space. When TEM is applied to tunnel geological surveys, the transmitter not only excites the induced eddy current in the surrounding rock in front of the tunnel face, but also in the surrounding rock behind the tunnel face. At this time, the signal received by the receiver is no longer the half-space signal, but the superposition of the full-space eddy current field signal. Because of the full-space effects, tunnel TEM is different from ground TEM, and needs to be studied separately.

2.2. Selection of input variables

The response curve of the tunnel was obtained by a TEM geological survey. The measured response curve consists of 20 or more sampling points. According to the relevant theoretical analysis [10], the response curve can be expressed as

$$V = A + A_1 e^{-a_1 t} + A_2 e^{-a_2 t} + \ldots + A_n e^{-a_n t} \tag{1}$$

where V is the response signal, t is the sampling time, A_i and a_i (i=1,2…,n) are undetermined coefficients, A is the combination of various constant terms, and e is the natural logarithm.

If 20 points are adopted as input variables, the training volume will be too large. Therefore, the response curve should be processed further to determine the input variables.

After the data acquired by detection have been homogenized, the characteristic curve is obtained, as shown in Figure 1. In Figure 1, WBB denotes a water-bearing body and UFSR denotes the uniform full-space surrounding rock. In Figure 1, the response curves of UFSR and WBB are compared. I_{cp} is a mathematical method used to divide the response of the UFSR from the response of the WBB, and can regulate abnormal data and highlight changes in the WBB. The specific formula is derived in a previous paper [11]. From the characteristic curve, the numerical characteristic points of the curve can be obtained. Through a linear transformation, seven digital feature parameters can be extracted from the acquired curve. The digital characteristic parameters mainly include the uplift point (UP), regression point (RP), maximum point (MP), maximum value

(MV), left time span (LTS), right time span (RTS), and total time span (TTS).

2.3. Selection of output variables

The selection of the output sample value corresponds to the geological condition parameters. In this study, TEM is mainly used to detect unfavorable geological conditions in tunnels, such as water-filled fault karst caves, as shown in Figure 2. These adverse geological conditions are reflected by the presence of bodies with low resistivity in the transient electromagnetic field. Therefore, the output variable is the conditional parameter of the low-resistance body. That is, the distance between the low-resistance body and the tunnel surrounding rock (L), and the radius (R), thickness (H), and resistivity (ρ) of the low-resistance body, as shown in Figure 2.

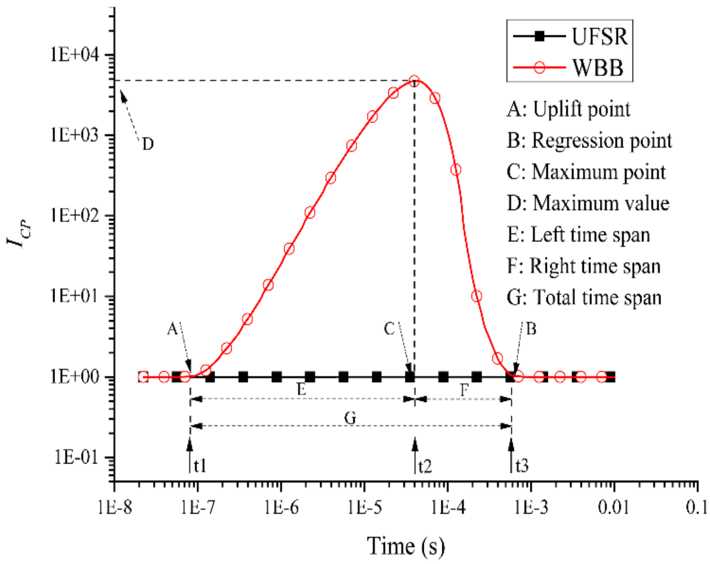

Figure 1. TEM characteristic curve.

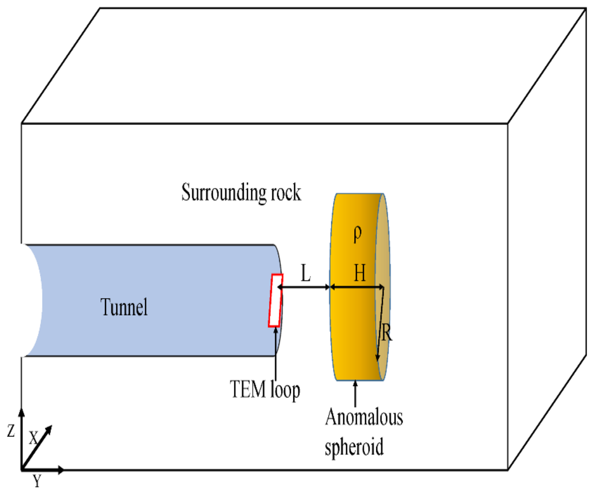

Figure 2. TEM detection schematic diagram.

3. Methodology

3.1. LSSVM

The SVM concept was developed from the optimal classification surface under the condition of linear separability. The basic idea is explained in Figure 3. The circles and stars represent two types of samples, H is the classification line, and H_1, H_2 are the classification interval lines, which identify the samples closest to H in each class. H_1 and H_2 are parallel to the classification line H. The equation of the classification line is given in Eq (2).

The classification plane with the most significant classification interval is the optimal classification plane. Moreover, the training sample points on H_1 and H_2 are support vectors. The problem of seeking the optimal classification surface can be expressed as the solution of a quadratic optimization problem. This optimization problem and its corresponding constraint conditions are given in Eq (3).

In the case of linear inseparability, if a relaxation term $\zeta \geq 0$ is added to Eq (3), the optimization problem and its corresponding constraint conditions are as shown in Eq (4). The nonlinear transformation function (5) is then used to transform this into a linear problem in high-dimensional space. Finally, the optimal classification surface is solved in the transformation space.

$$f(x) = x \cdot w + b = 0 \tag{2}$$

where w is the weight vector and b is the bias term.

$$\min J(w) = \frac{1}{2}\|w\|, y_i\left[\left(w \cdot x_j\right) + b\right] - 1 \geq 0,\ i = 1, \cdots, n \tag{3}$$

$$\min J(w, \xi) = \frac{1}{2}\|w\|^2 + C\left[\sum_{i=1}^{n} \xi\right], \sum_{i=1}^{n} \alpha_i y_i = 0, 0 \leq \alpha_i \leq C, i = 1, \cdots, n \tag{4}$$

where α_i are Lagrange multipliers, C is the regularization parameter, and ξ is the slack variable.

$$Z_j = \phi_j(x), j = 1, 2, \cdots, m \tag{5}$$

where $\phi(x)$ is the kernel space mapping function between the input space and the output space, which maps the input data points to a high-dimensional feature space [13].

In the feature space, a vector inner product operation is required to construct the optimal classification plane. Due to the high dimensionality of this space, it is difficult to derive this operation directly from Eq (5), so SVM methods adopt a kernel function K to replace the inner product operation in high-dimensional space, such as that given by Eq (6). Kernel functions can be used in training and testing. In conclusion, the dual optimization problem can be written as shown in Eq (7).

$$K\left(x_i, x_j\right) = \phi\left(x_i\right) \cdot \phi\left(x_j\right) \tag{6}$$

where K is the kernel function.

$$\max_{\alpha} L(\alpha) = \sum_{i=1}^{n} \alpha_i - \frac{1}{2} \sum_{i,j=1}^{n} \alpha_i \alpha_j y_i y_j K\left(x_i \cdot x_j\right) \tag{7}$$

where L is the Lagrangian function and α is the Lagrange multiplier.

Many SVM-based models have been proposed in this field, such as the LSSVM proposed by Suykkens [16]. The core idea of LSSVM is to replace the inequality constraint in classical SVM with an equality constraint to solve the optimization problem given in Eq (8).

The Lagrange polynomial of the above problem is of the form shown in Eq (9), and the optimization condition is given in Eq (10). The Mercer condition (11) is used to obtain the final fitting function (12). By adjusting the constraint conditions, the nonlinear problem can be approached more effectively.

$$\min_{w,\xi} J(w,\xi) = \frac{1}{2}\|w\|^2 + \gamma \sum_{i=1}^{n} \xi^2$$
$$y_i = (w \cdot \phi(x_i)) + b + \xi_i, i = 1, 2, \cdots, n \tag{8}$$

$$L(w,b,\xi,\alpha) = \frac{1}{2}w^T w + \frac{1}{2}C\sum_{i=1}^{m}\xi_i^2 - \sum_{i=1}^{m}\alpha_i \left\{ w^T\phi(x_i) + b + \xi_i - y_i \right\} \tag{9}$$

$$\frac{\partial L}{\partial w} = 0 \rightarrow w = \sum_{i=1}^{m}\alpha_i\phi(x_i)$$
$$\frac{\partial L}{\partial b} = 0 \rightarrow \sum_{i=1}^{m}\alpha_i = 0$$
$$\frac{\partial L}{\partial \xi_i} = 0 \rightarrow \alpha_i = C\xi_i$$
$$\frac{\partial L}{\partial \alpha_i} = 0 \rightarrow y_i = w^T\phi(x_i) + b + \xi_i \tag{10}$$

$$\Omega_{kj} = (\phi(x_k)\cdot\phi(x_j)) = K(x_k, x_j) \quad k, j = 1, \cdots, n \tag{11}$$

where Ω is the Mercer condition.

$$f(x) = \sum_{i=1}^{m}\alpha_i K(x, x_i) + b \tag{12}$$

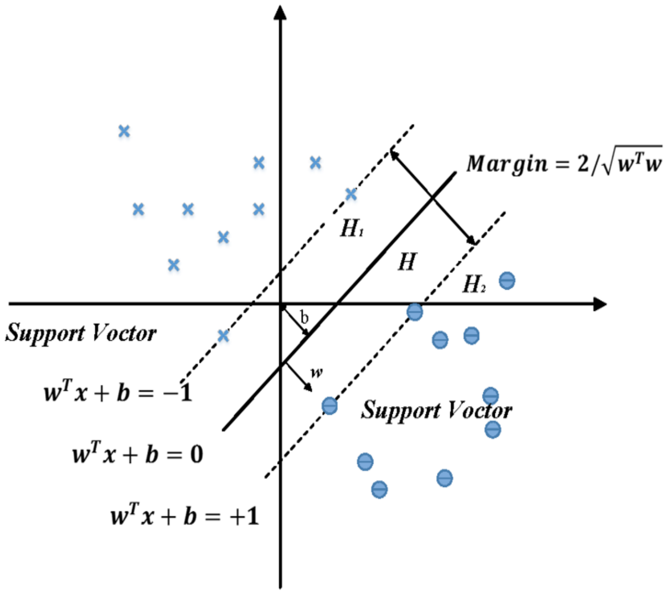

Figure 3. Schematic diagram of the SVM mechanism.

LSSVM is an improved form of SVM that provides better approximations for nonlinear problems. It is a useful tool for modeling and forecasting nonlinear systems. LSSVM requires fewer parameters and can find the optimal solution faster. However, the prediction effect is closely related to the kernel function parameters and regularization parameters. Therefore, in the process of computational optimization using LSSVM, the key steps are the selection of the kernel function type, kernel function parameters, and regularization parameters. Generally, the Gaussian kernel function has good anti-interference ability and is widely used. However, this kernel function is sensitive to its parameter values, so it is necessary to perform parameter optimization when using the Gaussian function.

TEM inversion is a multi-dimensional nonlinear problem with a complex inversion model. The Gaussian kernel function is selected to analyze the problem in this paper. Due to the parameter sensitivity of the Gaussian kernel function, the selection of parameters based on common experience may not be appropriate. Therefore, relevant algorithms are needed to optimize the two main parameters of the Gaussian kernel function, σ^2 and γ. Widely used optimization algorithms include genetic algorithms and particle swarm optimization (PSO). In this study, PSO is used to optimize LSSVM.

3.2. PSO algorithm

PSO is an intelligent algorithm inspired by the predation behavior of birds. The basic idea of this algorithm is to find the optimal solution through cooperation and information sharing among individuals in a group. The PSO algorithm has strong optimization ability. Moreover, it is easy to implement, has relatively few parameters, is conceptually simple, and converges rapidly. It has been widely used in function optimization, neural network training, and other fields.

The PSO algorithm includes two essential concepts: The individual best value (pbest) and the group best value (gbest). The former represents the optimal solution that an individual particle has found, whereas the latter represents the optimal solution of all particle extremum sets. The particle iterates to find the optimal solution. In each iteration, the particle updates itself by tracking two values (pbest, gbest). After finding these two optimal values, the particle updates its velocity and position according to Eqs (13) and (14). This is the standard form of PSO.

$$V_{i,N}(t+1) = w(t+1)V_{i,N}(t) + C_1 r_1 \left(X_{pbest,N} - X_{i,d}(t) \right) + C_2 r_2 \left(X_{pbest,N} - X_{i,d}(t) \right) \tag{13}$$

$$X_{i,N}(t+1) = X_{i,N}(t) + V_{i,N}(t+1) \tag{14}$$

where V is the velocity; $1 \le i \le m$; $1 \le t \le k$; m denotes the total number of particles; and k, t represent the maximum and current iteration numbers, respectively. C_1 and C_2 are positive constant acceleration coefficients, that is, the cognitive learning factor and the population learning factor, which represent the weights that each particle contributes to the individual and population optimal values. These two parameters are determined empirically, as discussed in section 4.1.

$$w(t) = w(1) - \left(w(1) - w(k) \right) t / k \tag{15}$$

$$f = MSE = \frac{1}{N} \sum_{i=1}^{N} \left(y - \overline{y} \right)^2 \tag{16}$$

where w is the inertia weight factor, which controls the influence of the previous velocity of the particle on the current velocity. When w is large, the global search ability of the algorithm is enhanced; when w is small, the local search ability is improved. The initial inertia weight is $w(1)$ and the inertia weight when the swarm has evolved to the maximum generation is $w(k)$. Measured and predicted values are denoted as y and ȳ, respectively. N is the total number of samples.

The PSO algorithm updates the index of particles through continuous evolution. After continued comparison, the optimal solution is reached. The optimization effect is influenced by the combination of initial parameters, namely, the particle swarm size, initial acceleration coefficients (C_1, C_2), and the number of iterations. Generally, parameters are selected at random based on experience, which makes the performance of PSO algorithms stochastic. To obtain the best optimization effect, the parameter selection should be optimized. The detailed optimization process is now described for the proposed PSO-LSSVM model.

3.3. Optimized PSO-LSSVM model

There are two essential parameters in LSSVM, namely the regularization parameter γ and kernel function parameter σ^2. The selection of these two parameters is typically based on experience, which introduces a large degree of randomness. To improve the prediction performance, two main parameters should be optimized.

The PSO algorithm is used to optimize the LSSVM model. However, the randomness of the initial parameter combination in the PSO algorithm leads to strong randomness in the optimization effect. Therefore, the PSO algorithm must be improved so as to select the optimal parameter combination and reduce its randomness. Orthogonal test design is an essential mathematical method in the study of multi-factor tests. The experimental factors are arranged reasonably and effectively, and optimization is achieved through the statistical analysis of the results. Therefore, orthogonal testing is used to determine the optimal combination of initial parameters for the PSO algorithm.

Firstly, 20% of the calculated samples are selected randomly as orthogonal test data (taking 20% of the data ensures the representativeness of the results while avoiding excessive calculations). Next, the horizontal range of each factor is selected, the orthogonal test table is designed, and the test group is chosen. Different test combinations are then substituted into the LSSVM model to calculate the output value. Finally, by analyzing the results, the optimal combination is selected as the initial parameter combination of PSO. This completes the improvement of the PSO algorithm.

The improved PSO algorithm is then used to optimize the LSSVM model (referred to as the optimization model), thus further improving the prediction effect of the model.

The model optimization steps are as follows:

(a). Select 20% of the data in the test samples. These data are used as samples to optimize the PSO algorithm;

(b). The sample level of the PSO parameters is determined, and the orthogonal test table is designed to obtain the PSO initial parameter combination;

(c). Take (γ, σ^2) as a particle swarm. Initialize the particle swarm;

(d). Obtain the first random value of the particle and train the LSSVM model. The initial iteration value is 1. After training, the target values of all particles are evaluated (the objective function is shown in Eq (16)). A smaller mean square error (MSE) indicates a more accurate prediction;

(e). The fitness values of the initial particle swarm are calculated and sorted, and the particle with the best fitness is selected. Set the current position of each particle to its own optimal position, and the current target value to the best target value. Set the optimal particle position and target value to be equal to the optimal global value;

(f). The location and speed of the particles are updated according to Eqs (13)–(15);

(g). After updating, the target values for all particles are evaluated;

(h). For each particle, compare its current target value with the best target value in its previous position. If the current target value is better than the previous best value, set this value as pbest. Compare each of the particles with gbest. If any particle scores higher than gbest, update the current value to gbest;

(i). Perform an iterative calculation and set the iteration termination conditions. If the number of iterations reaches the maximum number of iterations, terminate the calculation and proceed to step 10; otherwise, return to step 4;

(j). Obtain the optimal particle (γ, σ^2) and apply this to the LSSVM model to obtain the final output value;

(k). If the calculated results of the orthogonal scheme are not compared, the difference between the output values obtained by different scheme parameter combinations and the measured values will be compared. Analyze the optimal PSO parameter combination. If the results have been compared, proceed to step 12;

(l). Take all the data as samples, select the optimal PSO parameter combination, complete steps 3–10, and obtain the final output value.

The above procedure was implemented in Matlab 2016a. The overall flowchart is shown in Figure 4.

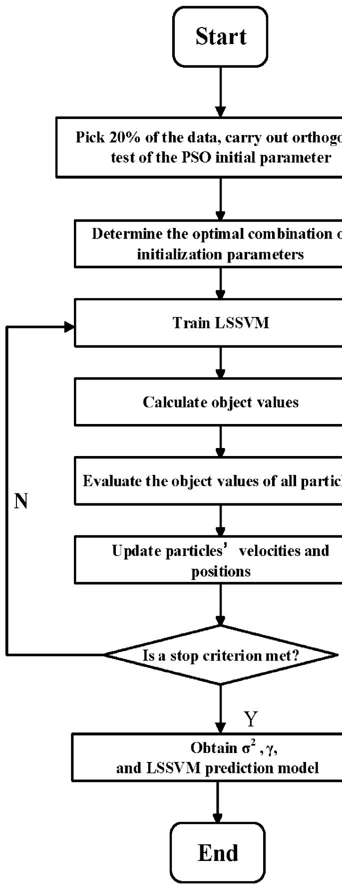

Figure 4. Flowchart of the PSO-LSSVM model for TEM.

4. Case study of tunnel TEM

Data training requires a large number of samples to ensure that the desired process can be fully learned, guarantee the correctness of the relationship, and produce accurate predictions. In this study, a large number of training samples were obtained through numerical simulations, which can be used for learning, training, and simulation of the model. A schematic diagram of the model is shown in Figure 5. To simulate an infinite space and prevent the reflection of electromagnetic waves at the boundary, an infinite cell boundary with a thickness of 20 m was set in the outer surrounding rock, as shown in Figure 5a. In the numerical model, the radius and height of the surrounding rock were set to 400 and 800 m, respectively. The resistivity of the surrounding rock was set to 1000 Ωm. The radius and thickness of the abnormal spheroid were determined according to the numerical experiment design table. The anomalous body and TEM loop were set inside the model. Due to the significant difference between the size of the full-space model and the size of the TEM coil, internal details of the loop and abnormal body were considered separately. The radius (R), thickness (H), and resistivity (R) of the abnormal spheroid and the distance from the TEM loop (L) are shown in Figure 5b. Through numerical modeling, different abnormal body distances, radii, thicknesses, and resistivities were applied to obtain the corresponding response curves. The extracted data were used to construct the sample set of numerical model results.

After obtaining simulation predictions, the difference between the predicted value and the target value was calculated, and the effect of simulation training was evaluated. Finally, two conventional machine learning methods were selected for comparison with the proposed PSO-LSSVM in an attempt to verify the inversion effect of the optimized model.

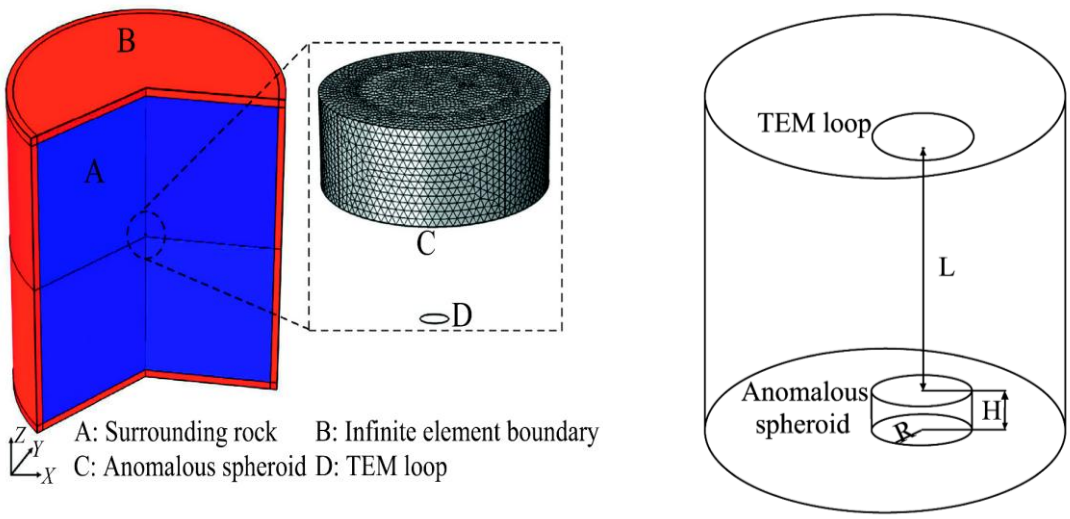

(a) Numerical calculation model (b) Schematic diagram of the model

Figure 5. Model of TEM.

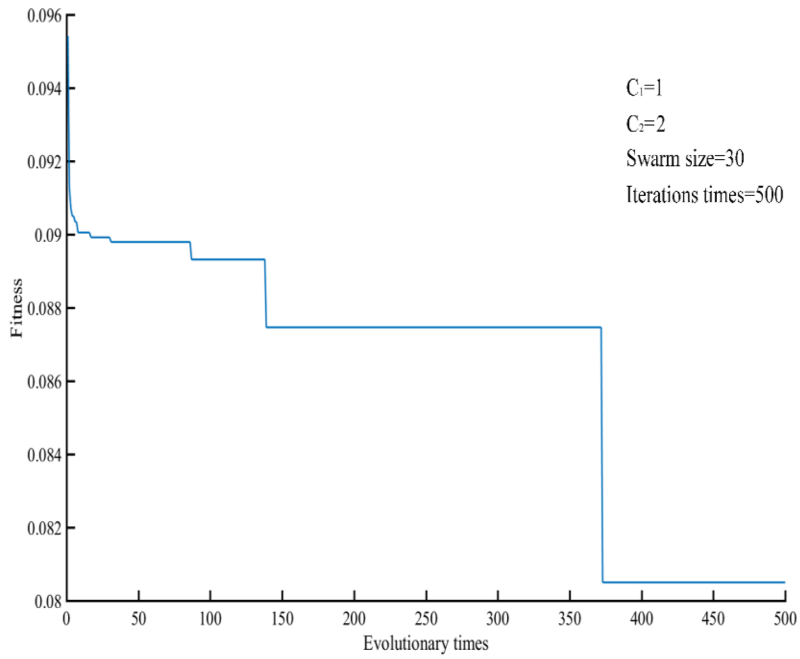

Figure 6. Evolution of global best fitness values.

4.1. PSO initial parameter orthogonal test

Orthogonal testing was carried out to select the optimal parameter combination for the PSO algorithm. The criterion was the MSE value, which represents the deviation between the predicted value and the measured value. The main initial parameters are the population size, initial acceleration coefficients C_1, C_2, and the maximum number of iterations.

According to Yamagami and Jiang [17], the population size is typically in the range 30–50. The maximum number of iterations determines the termination condition. A higher number is likely to achieve more accurate results, but at the cost of increased calculation time. Generally, 300–500 iterations is a reasonable maximum. A larger value of C_2 indicates stronger particle swarm awareness. Correspondingly, the “clustering” phenomenon of the particle swarm is more obvious, and the algorithm evolves quickly. However, this makes it easier to become trapped around local optima, a phenomenon known as premature convergence. A larger value of C_1 produces more independent particle behavior. Accordingly, the “dispersion” phenomenon becomes more obvious, but the algorithm evolves slowly and may terminate before a good solution has been found. Based on the relevant research [18−25], the range of both C_1 and C_2 is preliminarily set to [0, 2].

Based on the above, the influencing factors and orthogonal test table are presented in Tables 1 and 2.

According to the process of the orthogonal experiments, the mean and extreme differences in the target values were calculated, and the calculation results are given in Table 2. According to the range value R, it can be judged that the influence of each factor on the target value takes the following order: B > A > C > D. Therefore, C_1 has the most significant influence on the target value, followed by the swarm size and C_2; the maximum number of iterations has only a small influence on the output. The optimal combination was selected according to the results, and was determined to be (30, 1, 2, 500). After the PSO algorithm parameters were determined, the algorithm was used to optimize LSSVM.

Table 1. PSO initial parameter factor level.

Level	Swarm size	C_1	C_2	Number of iterations
1	30	0	0	300
2	40	1	1	400
3	50	2	2	500

Table 2. Orthogonal test design table.

Test number	Swarm size	C_1	C_2	Number of iterations	MSE
1	1	1	1	1	0.0580
2	1	2	2	2	0.0574
3	1	3	3	3	0.0574
4	2	1	2	3	0.0581
5	2	2	3	1	0.0390
6	2	3	1	2	0.0554
7	3	1	3	2	0.0582
8	3	2	1	3	0.0557
9	3	3	2	1	0.0574
K1	0.1728	0.1743	0.1691	0.1544	
K2	0.1525	0.1521	0.1729	0.1710	
K3	0.1713	0.1702	0.1546	0.1712	
k1	0.0576	0.0581	0.0564	0.0515	
k2	0.0508	0.0507	0.0576	0.0570	
k3	0.0571	0.0567	0.0515	0.0571	
R	0.0068	0.0074	0.0061	0.0056	

4.2. PSO-LSSVM model predictions

The initial parameter combination of the optimal PSO was obtained through orthogonal testing. Next, the optimization model was calculated. A Gaussian kernel function was used. The two main parameters of the Gaussian kernel function are γ and σ^2. Taking (γ, σ^2) as a particle swarm, the PSO algorithm was used to find the optimal solution. By calculating the particle fitness, the position and velocity of the particle were updated continuously, and the optimization was repeated. Finally, optimal values of $\sigma^2 = 0.22$ and $\gamma = 634.22$ were obtained.

The 125 groups of data were divided into 100 training sets and 25 test sets. After the operation, the fitness values of the particles were evaluated, as shown in Figure 6. The process was terminated when the maximum number of iterations was reached.

Figure 7 compares the predicted values and sample values. The upper and lower limits of the reasonable fluctuation range were set to 10% of the maximum value of the corresponding variable. If the predicted value exceeded the corresponding scale, the difference value was considered to be significant.

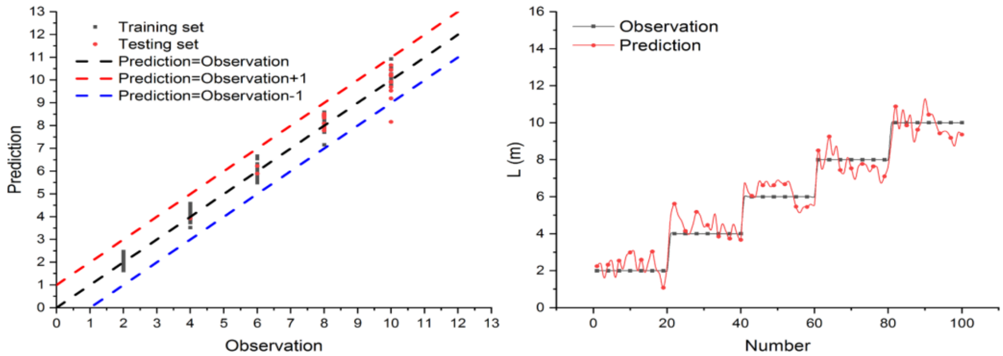

(a) Predicted values of L

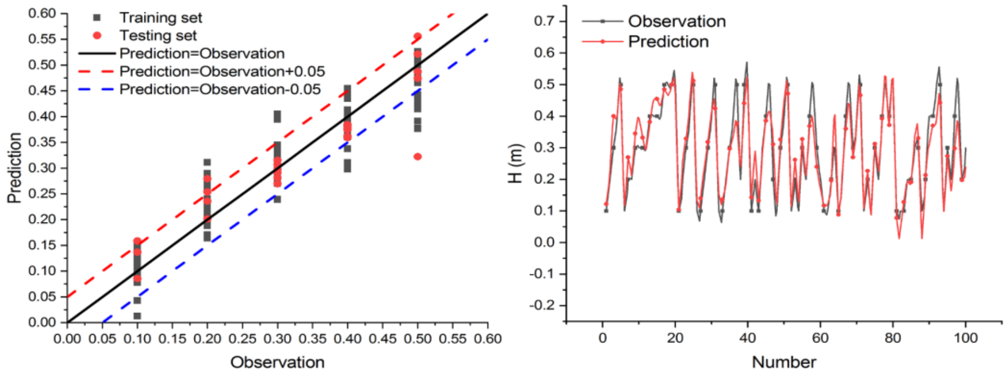

(b) Predicted values of R

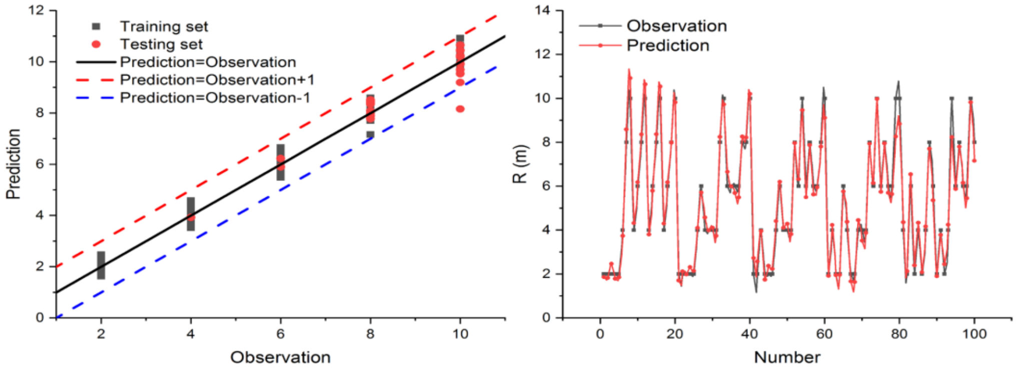

(c) Predicted values of H

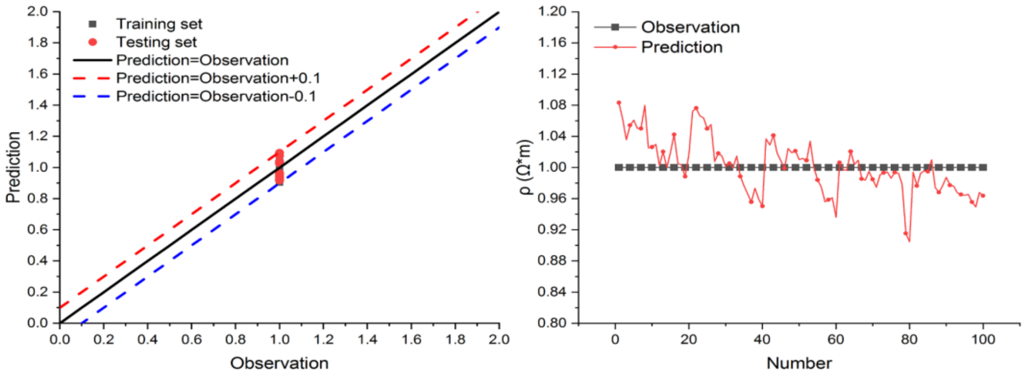

(d) Predicted values of ρ

Figure 7. Prediction curves under different conditions.

The differences in variable L are the smallest, and are typically less than 1, so the prediction results for this variable are the most accurate. The predicted values of H in the training process were slightly different from some of the sample data, and exceeded the reasonable fluctuation range. However, the predicted results are all within the reasonable range, indicating the general accuracy of the predicted values. Variable R performs well in both the training set and the test set, except that some points are slightly below the reasonable range. Variable ρ is set to a constant value of 1 in the experiment, and is not discussed here.

The comparison curves in Figure 7 show that the predicted values and the measured values exhibit consistent trends. The specific values fluctuate slightly, but generally remain within a reasonable range and have little influence on the final results. In summary, the predicted values are consistent with the actual values, indicating that the model training effect is excellent and accurate predictions can be realized.

4.3. Comparative analysis of different models

To verify the inversion prediction effect of the optimization model, two conventional models (unoptimized LSSVM and a backpropagation (BP) neural network) were used for inversion. By comparing the prediction performance of each model, the most appropriate was determined. The results were then compared with those from the proposed optimization model.

In analyzing the performance of an inversion model, the accuracy of the predicted values, stability of the model, and generalization ability must be considered. The accuracy was analyzed by comparing the MSE of the predicted values, model stability was analyzed in terms of the MSE variation, and the generalization ability was analyzed through the difference between the training set and the test set. To analyze the stability of the model, multiple calculations were required. Considering the calculation time and the processing power of the computer, 10 calculations were performed for each model. The results were then aggregated and analyzed accordingly.

The only significant difference between the unoptimized LSSVM model and the optimized model concerns the randomness of the parameter selection. Thus, the specific mechanism of this model is not described in detail. The BP model has one hidden layer and an output layer, as shown in Figure 8. There are 10 units, seven input variables, and four output variables. The training and test data were consistent with those adopted in the previous experiments.

After 10 training predictions, the MSE was evaluated. Compared with the variance of the optimization model, the corresponding MSE curve is shown in Figure 9. It can be seen that the BP model has a large MSE during the 10 training sessions. This indicates that the model undergoes large fluctuations and is not particularly stable. Moreover, the error with the test sets is much larger than that with the training sets, which indicates weak generalization ability and a poor inversion effect. The MSE value of the unoptimized LSSVM model is relatively small. However, repeated fluctuations appear in the results with the training set and test set, indicating the randomness and instability of this model. The optimized model gives the smallest MSE values, and after several initial tests, the error remains relatively stable, without repeated oscillations. This indicates that the model guarantees overall stability and accuracy.

In conclusion, considering the accuracy of prediction, generalization ability, and stability, the optimized model is superior to both the BP model and the unoptimized LSSVM model.

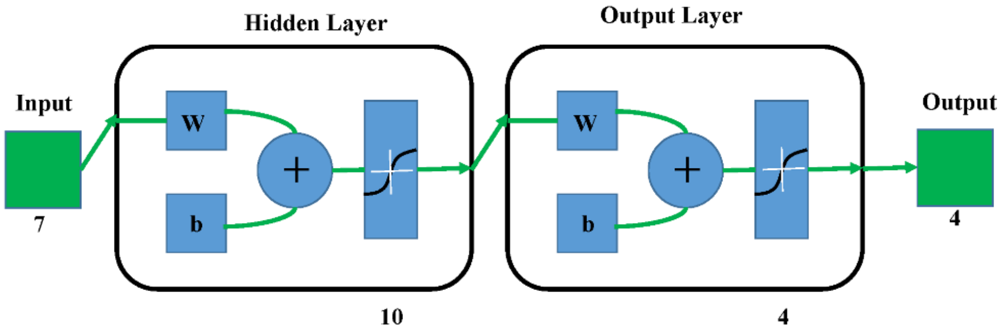

Figure 8. BP neural network structure.

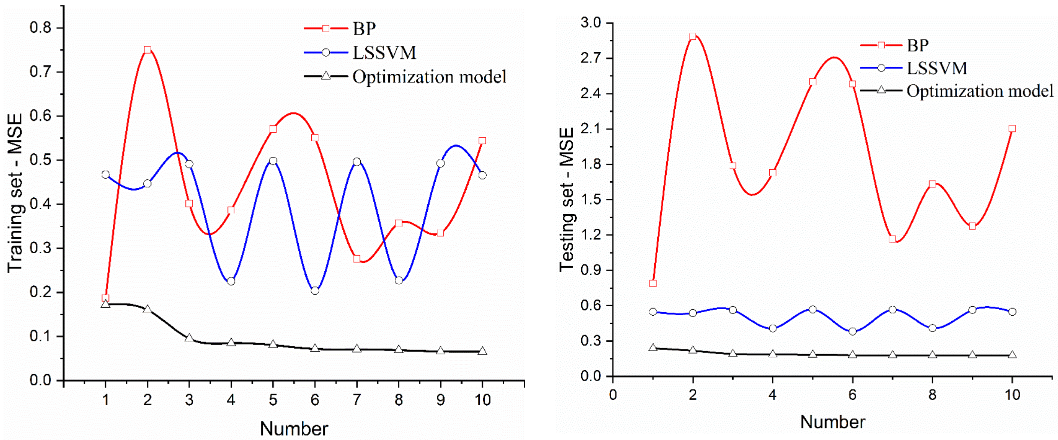

(a) Training set MSE (b) Testing set MSE

Figure 9. Error comparison between models.

4.4. Laboratory model test verification

Through learning and trial calculations using the data obtained from the numerical simulations, the optimized PSO-LSSVM model has been found to achieve a good prediction effect. Compared with the unoptimized LSSVM and BP model, it offers significantly improved generalization ability, stability, and accuracy. However, the application of the above optimization model is based on numerical simulations, and the application effect in practical engineering should be further verified. It is relatively difficult to detect anomalous bodies of different sizes and generate the associated statistics in practical engineering, but laboratory model tests can simulate different situations and better reflect the real situation. Thus, a scale model test was conducted.

The electromagnetic response is the fundamental principle of TEM. It is known that TEM is particularly sensitive to changes in resistivity, and the significant resistivity differences allow TEM to detect water-bearing abnormal bodies in tunnel rock mass. Therefore, the resistivity characteristics of rock mass and a water-bearing abnormal body should be considered in the laboratory model test. Saltwater was used to simulate the tunnel rock mass, and graphite was used to simulate the abnormal body. The depth of the rock mass, size of the abnormal body, and distance from the detected position to the abnormal body were simulated by adjusting the volume of brine, size of the graphite column, and position of the coil, respectively. A schematic diagram of the laboratory test model is shown in Figure 5b. The design of the test scheme is described in Table 3.

The equipment involved in the laboratory test model is shown in Figure 10, and the corresponding parameters are introduced as follows:

Detection instruments: PRO TEM 47 (including transmitter, transmitter loop, receiver, receiver loop, and signal amplifier);

Water tank: length × width × height = 100 × 100 × 100 (cm);

Brine: Concentration 5%; resistivity 0.1 Ωm;

Graphite column A: radius × height = 10 × 20 (cm), resistivity 1×10^{-5} Ωm;

Graphite column B: radius × height = 10 × 10 (cm), resistivity 1×10^{-5} Ωm;

Graphite column C: radius × height = 4 × 10 (cm), resistivity 1×10^{-5} Ωm.

The detection data obtained through the laboratory model test are presented in Table 4. The detection data were input to the optimization model for prediction, and the corresponding prediction values were obtained. The predicted values and actual test values were statistically analyzed, and the results are shown in Figure 11. The predictive values given by the model are clearly similar to the actual values of L, H, R, and ρ. When the values of L and R change significantly, the predicted values also change, but the amplitude of the change is smaller and there is some hysteresis. For variables H and ρ, which have small change amplitudes, the change in the predicted values is also small and relatively stable. In general, the predicted values given by the model are accurate, and the trends are consistent with the actual situation. Thus, the proposed hybrid PSO-LSSVM model is an effective method for solving TEM inversion problems.

Table 3. Design table of the laboratory model test.

No.	L (cm)	H (cm)	R (cm)	ρ (Ωm)
1	10	20	4	1
2	10	20	10	1
3	10	10	4	1
…	…	…	…	…
8	4	10	10	1

Table 4. Detection data.

No.	UT	RT	MT	MV	LTS	RTS	TTS
1	6.58	4.79	5.39	0.58	1.29	0.57	1.85
2	6.33	4.29	5.04	1.78	1.38	0.71	2.08
3	6.67	5.04	5.69	0.28	1.09	0.62	1.70
…	…	…	…	…	…	…	…
8	6.83	4.49	5.39	2.54	1.58	0.88	2.45

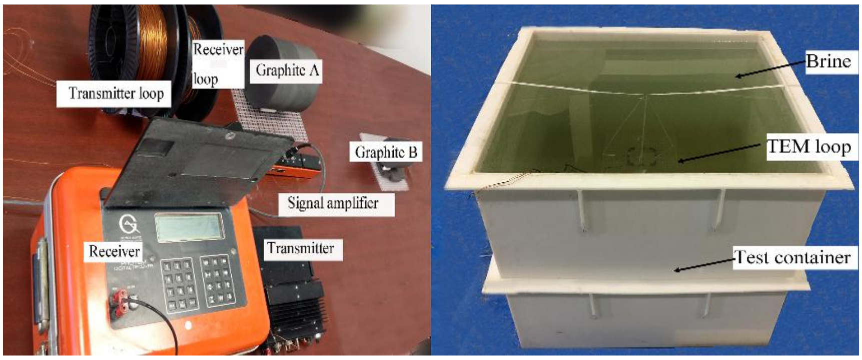

Figure 10. Laboratory test model.

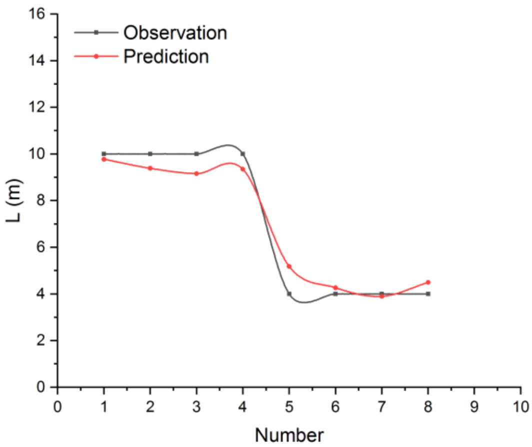

(a) Predicted values of L

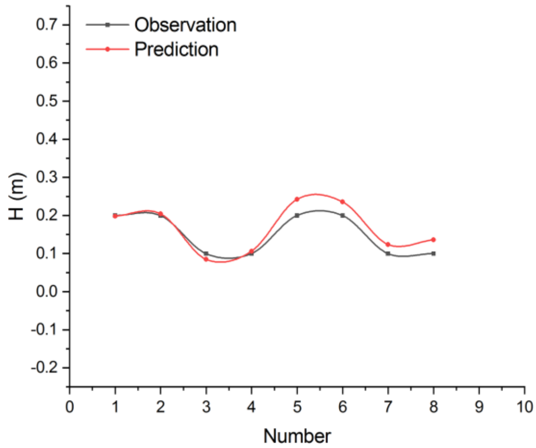

(b) Predicted values of R

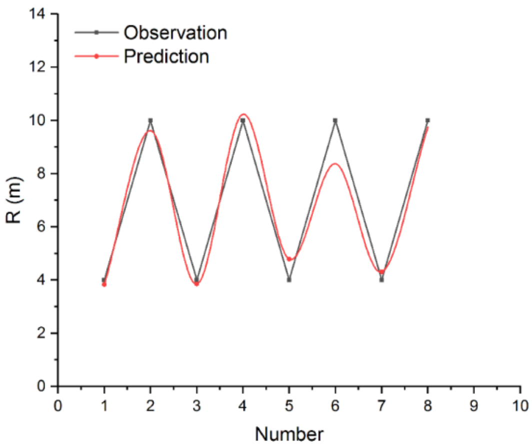

(c) Predicted values of H

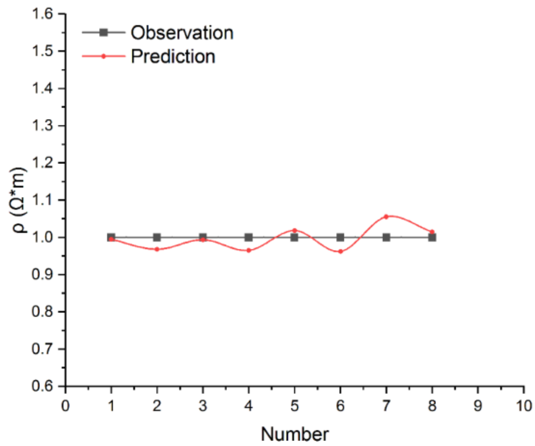

(d) Predicted values of ρ

Figure 11. Comparison of predictions with actual values.

5. Conclusions and discussions

TEM is an accurate and effective method for detecting geological hazards in tunnels, but the deficiency of the inversion method limits its application. An effective and accurate inversion method would promote the application of TEM and realize accurate early warning of geological disasters.

Thus, an optimized inversion model has been proposed in this paper. The optimized PSO-LSSVM model has been applied to solve the inversion problem of tunnel TEM detection, and the main conclusions are as follows:

The PSO algorithm is a useful optimization algorithm, but the selection of initial parameters is essentially random, which affects the optimization performance. Through orthogonal test analysis, the randomness of PSO can be reduced and its optimization performance improved.

The prediction effect of the LSSVM model mainly depends on the regularization parameter σ^2 and the kernel function parameter γ. Using the improved PSO algorithm, the optimal selection of these two parameters enables the optimization of the PSO-LSSVM model and the evaluation of the corresponding prediction results.

Comparing the prediction results given by the optimized model with those from an unoptimized LSSVM and a BP neural network model, it was found that the generalization ability, stability, and accuracy of the optimized model were superior to those of the other models. A laboratory model test offered further verification of the practical applicability of the proposed optimization model. Thus, the optimization model is an effective TEM inversion method for tunnels.

However, this study and the proposed method have the following problems that need to be overcome.

(a) This paper describes an exploratory study on TEM inversion, and thus considers a simplified anomalous body and only certain parameters (namely, L, H, R, and ρ). However, these four parameters are too simple to satisfy the high-precision requirements of practical engineering. Therefore, it is still necessary to study the parameters of the abnormal body in detail and to form a complete detection system combining various methods prior to application in engineering scenarios.

(b). The initial parameters of the PSO algorithm are determined according to the application cases of existing PSO algorithms in civil engineering, and the optimal values are determined by orthogonal testing. In subsequent research, relevant TEM detection data should be accumulated through a large number of experiments, and the parameter selection should be combined with the inversion results of classical experimental functions. This would enhance the applicability of the proposed hybrid PSO-LSSVM parameters in the TEM inversion field.

Acknowledgments

The National Natural Science Foundation of China (grant nos. 51278423 and 51478395) are acknowledged for their financial support of this research.

The authors would also like to thank the two anonymous reviewers for their helpful and constructive comments.

Conflicts of interest

All authors declare no conflicts of interest in this paper.

References

1. E. D. Jens, A. Esben, J. Flemming, The application of the transient electromagnetic method in hydrogeophysical surveys, *J. Appl. Geophys.*, **53** (2003), 181–198.

2. A. Kanta, P. Soupios, P. Barsukov, M. Kouli, Aquifer characterization using shallow geophysics in the Keritis Basin of Western Crete, Greece, *Environ. Earth Sci.*, **70** (2013), 2153–2165.
3. D. Kalisperi, M. Kouli, F. Vallianatos, A transient electromagnetic (TEM) method survey in north-central coast of Crete, Greece: Evidence of seawater intrusion, *Geosciences*, **8** (2018), 2076−3263.
4. F. Vallianatos, M. Kouli, D. Kalisperi, Evidence of hierarchy in the complex fractured system of geropotamos (Crete, Greece), as extracted from transient electromagnetic responses, *Pure Appl. Geophys.*, **175** (2018), 2895−2904.
5. D. A. Pavlov, M. S. Zhdanov, Analysis and interpretation of anomalous conductivity and magnetic permeability effects in time domain electromagnetic data, *J. Appl. Geophys.*, **46** (2001), 217–233.
6. M. Y. Cheng, Y. W. Wu, L. Chen, Risk preference-based support vector machine inference model for slope collapse prediction, *Autom. Constr.*, **22** (2012), 175–181.
7. C. Zhou, L. Y. Ding, Y. Zhou, Hybrid support vector machine optimization model for prediction of energy consumption of cutter head drives in shield tunneling, *J. Comput. Civ. Eng.*, **33** (2019), 04019019.
8. H. F. Sun, X. Li, X. S. Lu, Transient electromagnetic responses in tunnels with strong interferences and the correcting method: A TBM example, *Chin. J. Geophys.*, **59** (2016), 4720–4732.
9. G. Q. Xue, Y. J. Yan, X. Li, Q. Y. Di, Transient electromagnetic S-inversion in tunnel prediction, *Geophys. Res. Lett.*, **34** (2007).
10. D. M. Tan, *Research on Theory and Application for Advanced Prediction of Water by Whole Space Transient Electromagnetism*, Master thesis, Southwest Jiaotong University, 2009.
11. W. P. Qian, T. Y. Qi, X. Liang, S. J. Qin, Z. Y. Li, Y. Li, Vehicle-borne transient electromagnetic numerical characteristic parameter of water-bearing body behind tunnel linings, *Math. Probl. Eng.*, **2020** (2020), 8514913.
12. S. E. Cho, Probabilistic stability analyses of slopes using the ANN-based response surface, *Comput. Geotech.*, **36** (2009), 787–797.
13. X. H. Xue, Prediction of slope stability based on hybrid PSO and LSSVM, *J. Comput. Civ. Eng.*, **33** (2019), 04016041.
14. J. Rostami, Performance prediction of hard rock tunnel boring machines (TBMs) in difficult ground, *Tunn. Undergr. Space Technol.*, **57** (2016), 173–182.
15. L. M. Zhang, X. G. Wu, H. P. Zhu, Performing global uncertainty and sensitivity analysis from given data in tunnel construction, *J. Comput. Civ. Eng.*, **31** (2017), 040170.
16. J. A. K. Suykens, J. Vandewalle, Least squares support vector machine classifiers, *Neural Process. Lett.*, **9** (1999), 293−300.
17. Y. Yamagami, J. C. Jiang, A search for the critical slip surface in three-dimensional slope stability analysis, *Soils Found.*, **37** (1997), 1–16.
18. J. Kennedy, R. Eberhart, Particle swarm optimization, in *ICNN'95—International Conference on Neural Networks*, IEEE, 1995.
19. Y. H. Shi, R. Eberhart, A modified particle swarm optimizer, in *1998 IEEE International Conference on Evolutionary Computation Proceedings. IEEE World Congress on Computational Intelligence*, IEEE, 1998.
20. R. Y. Ma, L. L. Yang, Z. C. Zhang, Analysis the characteristic of C1, C2 based on the PSO of iterative shift and trajectory of particle, *Math. Comput.*, **4** (2013), 109–115.

21. C. Elegbede, Structural reliability assessment based on particle swarm optimization, *Struct. Saf.*, **27** (2005), 171–186.
22. M. Y. Cheng, N. D. Hoang, Risk score inference for bridge maintenance project using evolutionary fuzzy least squares support vector machine, *J. Comput. Civ. Eng.*, **28** (2014), 04014003.
23. T. Lee, L. Thomas, The transient electromagnetic response of a polarizable sphere in a conducting half space, *Geophys. Prospect.*, **40** (1992), 541–563.
24. H. M. Lin, S. K. Chang, J. H. Wu, C. H. Juang, Neural network-based model for assessing failure potential of highways lopes in the Alishan, Taiwan area: Pre-and post-earthquake investigation, *Eng. Geol.*, **104** (2009), 280–289.
25. M. N. Nabighian, Quasi-static transient response of a conducting half-space—An approximate representation, *Geophysics*, **44** (1979), 1700–1705.